Journal of Hydroscience and Hydraulic Engineering
Vol. 11, No. 1, May, 1993, 31-40

NUMERICAL SIMULATION OF BED-LOAD TRANSPORT IN UNSTEADY UNIFORM FLOW

By

Hitoshi GOTOH

Research Associate, Department of Civil Engineering, Kyoto University
Yoshida Honmachi, Sakyo-ku, Kyoto, 606, Japan

Tetsuro TSUJIMOTO

Associate Professor, Department of Civil Engineering, Kanazawa University
2-40-20, Kodatsuno, Kanazawa, 920, Japan

and

Hiroji NAKAGAWA

Professor, Department of Global Environmental Engineering, Kyoto University
Yoshida Honmachi, Sakyo-ku, Kyoto, 606, Japan

ABSTRACT

Numerical simulation of the bed-load transport is executed on the basis of the equation of motion of bed-load particle, to evaluate the characteristics of the moving period which represents the unsteady bed-load transport system. The results of moving period by the present simulation are compared with the experiments under the oscillation-current coexisting flow. The characteristics of mean, standard deviation and probability density of the moving period are discussed. The time variation of the deposit rate and the sediment discharge under oscillation-current coexisting flow are simulated. Furthermore the sediment discharge due to the wave action is also simulated. The agreement between the simulation and the experiments indicates that the transport process can be well simulated by the present method.

INTRODUCTION

The bed-load transport process is characterized by the irregular motion of particles, and thus the stochastic model which describes the irregularity of the bed-load motion is essential to establish the bed-load transport formula. The irregular motion of particles has two aspects: (i) the quick motion and (ii) the irregular resting duration between the successive two moving steps. Einstein (1) proposed the stochastic model of bed-load transport which described the probabilistic characteristics of the bed-load motion. Nakagawa & Tsujimoto (2) proposed a generalized formulation of Einstein's model, namely the Eulerian stochastic model, which is formulated as a convolution integral constituted by pick-up rate and step length; it is very useful means to explain the various types of alluvial phenomena under the non-equilibrium condition. In their model, the pick-up rate was estimated from the mechanism of the bed-load particle's motion, while the step length was estimated by the semi-empirical model. The pick-up rate is governed by the local velocity-field around the particle on bed; on the other hand, the step length is affected by the variation of the velocity along the path of particle. Hence it is important to consider a hysteresis of the particle for accurate calculation of bed-load motion. Furthermore, the hysteresis of the bed-load motion is affected mainly by the irregular collisions with the protrusions on bed.

In order to estimate the step length, Nakagawa, Tsujimoto & Hosokawa (5) carried out the numerical simulation of the bed-load motion based on the equation of sliding motion, with focusing upon the collision process with the protrusions distributed at an irregular spacing on a rough bed. They divided the bed-load transport process into two subprocesses illustrated in Fig. 1: (A) the collision process with the protrusion on bed; and (B) the moving process without collision. To describe the characteristics of the collision (subprocess (A)), they took into account the motion of a particle rolling over protrusions

after perfectly elastic collision with the protrusion. The subprocess (B) is discussed as a sliding motion. On the other hand, Tsujimoto & Nakagawa (6) executed the simulation of the two-dimensional irregular successive saltation; in their simulation, the transport process is divided into two subprocesses: (i) the collision and repulsion with the bed-material particles, and (ii) the saltation as the moving process apart from a bed. Sekine & Kikkawa (8) performed the simulation of three-dimensional successive saltation by adopting the same kind of the concept as Tsujimoto & Nakagawa's. They found that the difference of the result of the three-dimensional model from that of the two-dimensional one is so small that most of the characteristics of the bed-load transport are well estimated by the two-dimensional simulation.

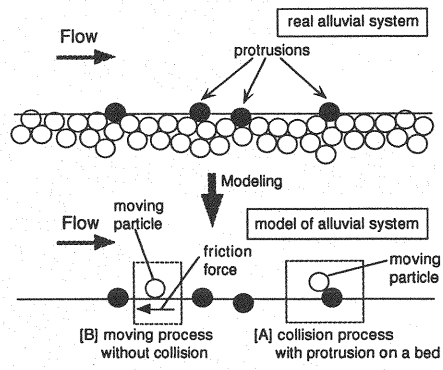

Fig. 1 Illustration of bed-load transport

All of these previous studies treated the bed-load transport in steady flow, while the hydraulic condition is not steady in the real alluvial system, in other words, the fluctuation of hydrodynamic forces acting on the bed-load particles distribute in wide range of frequency. Among them, high-frequency fluctuation, namely turbulence, should be treated by considering the dynamic response of the bed-load transport system to it; while the particle motion under low-frequency fluctuation, like a tidal current or a flood, can be explained well under the quasi-steady assumption. Under the intermediate-frequency fluctuation, which is in the same order as the characteristic time scale of the bed load transport, or the moving period, the sediment motion is so sensitively affected by the unsteadiness of the flow that it should be treated as the non-equilibrium transport process along a time axis.

In the experiment, sampling number of particles depends on the pick-up rate at each phase, and it is difficult to collect a sufficient number of samples at the phase with small pick-up rate. In other words, the sampling number in the experiment is different in each dislodging phase of particle, and the reliability of experimental data for each phase is not same. To avoid such a deficiency of the experiment, the numerical simulation which can easily collect the enough number of data with the equal reliability should be conducted.

The accuracy of the simulation mostly depends on whether the elementary event of simulated phenomena is properly chosen or not. The elementary event of an alluvial system is the motion of an individual particle, which follows evidently to Newtonian mechanics. The general aspect of the bed-load transport process should be expressed as an ensemble set of the motion of an individual particle. From this point of view, the numerical simulation should be positively utilized in estimating the detail mechanism of the alluvial system that is difficult to be investigated by physical experiment. In this study, by considering such advantages, the numerical simulation is utilized to discuss the characteristics of bed-load motion at unsteady flow.

In this paper, the bed-load transport process under unsteady and uniform flow is simulated based on the equation of sliding motion, and the characteristics of the moving period of particles are evaluated. The time series of the deposit rate and the sediment discharge are calculated by using the evaluated moving period. The results of the simulation are compared with the experimental data of the deposit rate and sediment discharge under the oscillation-current coexisting flow, which is unsteady-uniform flow. The simulation is also applied to the experiments of Sawamoto & Yamashita (7) on the bed-load transport due to the wave action to discuss the applicability of the model to the wave driven sediment transport.

SIMULATION MODEL

The bed-load transport process is divided into two subprocesses: (A) the collision process with protrusion on bed, and (B) the moving process without collision (Nakagawa, Tsujimoto & Hosokawa (5)). This simulation is conducted following this concept. The outline of the simulation model is explained hereafter. For the simplicity, the two-dimensional motion is considered in both subprocesses.

Collision process of a bed-load particle with protrusion on bed:

The situation illustrated in Fig. 2 is assumed as a collision process. By considering the changes of the momentum and the angular momentum during the process of collision, the relation between the initial speed of particle, u_{in}, and the speed of particle after a collision, u_{out}, is given as follows:

$$\frac{u_{out}}{\sqrt{gd}} = \sqrt{\left(\frac{1+4k^2/d^2-2\Delta_*}{1+4k^2/d^2}\right)^2 \frac{u_{in}^2}{gd} - 2\Delta_* B_*} \qquad (1)$$

$$B_* = \frac{\sigma/\rho - 1}{(\sigma/\rho + C_M)(1+4k^2/d^2)} \qquad (2)$$

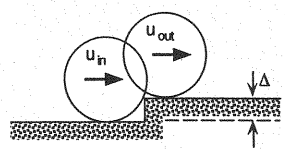

Fig. 2 Shematic figure of collision

in which d=diameter of particle; g=gravitational acceleration; σ=mass density of particle; ρ= mass density of fluid; C_M= added mass coefficient; and k=radius of gyration defined as follows:

$$k = \sqrt{\frac{I_G}{M}} \quad ; \quad I_G = \frac{2}{5}\rho\left(\frac{\sigma}{\rho} + C_M\right) A_3 d^5 \qquad (3)$$

in which I_G=moment of inertia; and A_3=three dimensional geometric coefficient. The probabilistic varieties of collision is governed by the distribution of the dimensionless height of protrusion, $\Delta_* \equiv \Delta/d$ (Δ=height of the protrusion), which can be approximated by an exponential distribution (Nakagawa et al. (5)). Then, the probability density function of Δ_* is written as follows:

$$f_H(\Delta_*) = \frac{1}{\Delta_{*0}} \exp\left(-\frac{\Delta_*}{\Delta_{*0}}\right) \quad ; \quad \Delta_{*0} = 0.3 \qquad (4)$$

When the moving particle collides with protrusions, the height of protrusions are given by Eq. 4 with generating the random numbers, and the speed of particle u_{out} is calculated by Eq. 1. To simplify the procedure, Nakagawa et al. (5) deduced the transition probability function which represents the relation between u_{in} and u_{out} as follows:

$$h(u_{out}^* | u_{in}^*) = \frac{1}{\Gamma(4)} \Xi_h^4 u_{out}^{*3} \exp(\Xi_h u_{out}^*) \quad ; \quad \Xi_h = \frac{4}{0.08 u_{in}^{*2} + 0.3 u_{in}^*} \qquad (5)$$

$$u_{in}^* = \frac{u_{in}}{\sqrt{gd}} \quad ; \quad u_{out}^* = \frac{u_{out}}{\sqrt{gd}} \qquad (6)$$

where $\Gamma()$= gamma function.

Moving process without collision:

The equation of the sliding motion:

$$\rho\left(\frac{\sigma}{\rho} + C_M\right) A_3 d^3 \frac{du_p}{dt} = \frac{1}{2} C_D \rho |u - u_p| (u - u_p) A_2 d^2 + \rho(1 + C_M) A_3 d^3 \frac{du}{dt} - g\left(\frac{\sigma}{\rho} - 1\right) A_3 d^3 \mu_f \qquad (7)$$

is adopted, where u_p=the speed of particle in the longitudinal direction; x_p=the coordinate in longitudinal direction; C_D=drag coefficient; and A_2=two-dimensional geometric coefficient. The coefficient of the kinetic friction, μ_f, given by Nakagawa et al. (5) is:

$$\mu_f = \frac{1}{2} \frac{\mu_{f0}}{(u_p/\sqrt{gd})^2 + 0.5} \quad ; \quad \mu_{f0} = 1.8 \qquad (8)$$

where μ_{f0}=coefficient of static friction.

Procedure of simulation:

Figure 3 shows the procedure of the simulation. Firstly, the position of protrusions are determined by generating random numbers with considering the statistical characteristics of the spatial distribution of protrusions investigated experimentally by Nakagawa et al. (5). The spacing of protrusions on an alluvial bed follows to the gamma distribution, the statistical properties of which are as follows:

$$x_{pr} = (5.0 \sim 7.0)d \quad ; \quad \alpha_x = 0.6 \sim 0.7 \qquad (9)$$

where x_{pr}=mean interval of two neighboring protrusions $\{x\}$; and α_x=variation coefficient of $\{x\}$.

Secondly, the initial condition of particle's motion is set as follows:

$$x_p = 0, \quad u_p = 0 \quad ; \quad \text{at} \quad t = 0 \qquad (10)$$

Thirdly, the motion of the particle is traced by solving Eq. 7 with Runge-Kutta-Verner method. In the process of tracing particle, the collision assessment is performed by comparing the position of the moving particle with that of protrusions. When the collision occurs, the speed of particle just after collision u_{out} is calculated by Eqs. 5 and 6.

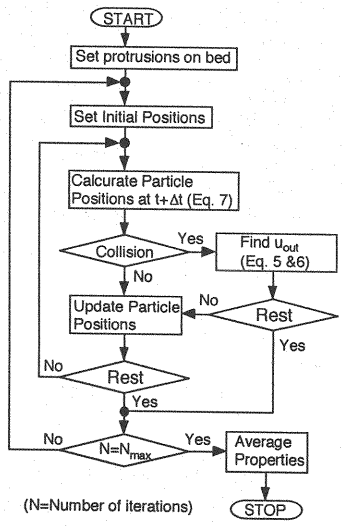

Fig. 3 Procedure of simulation

In the bed-load transport process under unsteady flow condition, two types of rest condition exist; (i) the rest due to the sudden momentum loss by collision, and (ii) the rest caused by the decrease of the hydrodynamic force beneath the critical shear stress. The rest assessment is done after collision. When the following condition (rest condition (i)) is satisfied, the particle is regarded as resting on bed:

$$u_{out} \le \beta_1 u_{in} \quad ; \quad \beta_1 = 0.1 \qquad (11)$$

where β_1= empirical constant related to the imperfect elasticity of collision. In the derivation of Eqs. 5 and 6, the perfectly elastic collision is supposed, though the real collision is not perfectly elastic. The imperfect elasticity of collision is considered by introducing Eq. 11. When the rest condition (i) is not satisfied, the position and speed of particle is updated, and the other rest assessment (rest condition (ii)) is performed. When the condition (ii) is not satisfied, the trace of particle is continued; while the condition (ii) is satisfied, total number of the traced particle, N, is counted. This procedure is continued until N becomes the maximum number of the iterations N_{max}. The coefficients adopted in this simulation are as follows: C_M=0.5, C_D=0.4, A_2=π/4; and A_3=π/6 which are frequently employed in the previous studies (3).

APPLICATION OF SIMULATION TO OSCILLATION-CURRENT COEXISTING FLOW

The results of the simulation are compared with the experiments under the oscillation-current coexisting flow conducted by Nakagawa, Tsujimoto & Gotoh (4). A series of experiments was carried out in a U-tube type oscillating water tunnel illustrated in Fig. 4. This is made of acrylic resin and has the working section is 180cm long, 10cm high and 40cm wide. Through acrylic hatches located above the central part of the working section, the access to the inside of the water tunnel is possible. The motion of the particle was recorded by a CCD video camera located above the working section. The test section (20cm×20cm) was set at the central part of the working section so that the three-dimensional effect of flow on the motion of particles was avoided. The damping of the oscillation was inevitable, because the experimental apparatus has no motor-driven mechanism to maintain the os-

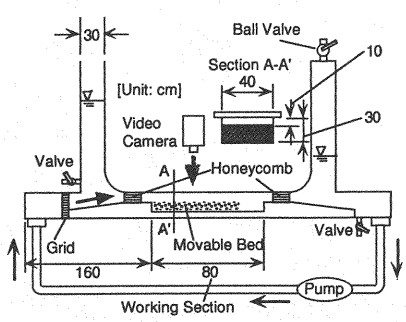

Fig. 4 Experimental apparatus

cillation. To avoid the effect of damping, the motion of the particles were analyzed for the one-cycle just after the beginning of the oscillation. Table 1 shows the experimental conditions. Test particle was spherical plastic one with the specific gravity 1.48 and the diameter 4 mm. The current velocity was set at the magnitude just below the threshold of particle motion so that no particle moved before beginning of the oscillation. Fig. 5 shows the time series of current velocity measured by a micro propeller currentmeter of 3mm-diameter. A broken line is a mean velocity variation through a lowpass filter estimated by the discrete Fourier transform. In the present simulation, the measured velocity was utilized for the calculation of the acting force on moving particles.

Table 1 Experimental condition

	Run 1	Run 2
Diameter of the particle d(cm)	0.4	
Relative density of the particle σ/ρ	1.48	
Amplitude of the oscillating velocity U_w(cm/s) at y=d/2	41.01	43.74
Mean velocity of the current u_c (cm/s)	18.0	18.0
Ratio of U_w to u_c (U_w/u_c)	2.28	2.43
Period of the oscillation T(s)	4.0	4.0

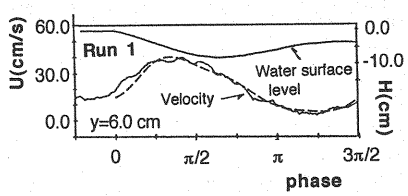

Fig. 5 Current velocity

Figure 6 shows the change of mean moving period with the dislodging phase of particle. The experimental results were compared with the mean moving period simulated by the stochastic model. The calculated result by deterministic model, in which the bed-load transport process is treated as the sliding motion without collision, is also shown in the figure. Although both stochastic model and deterministic model express well the fundamental feature that the mean moving period decreases with the increase of the particle's dislodging phase, the deterministic model shows the overestimation when the particle's dislodging phase is small. The difference of the result between the stochastic model and the deterministic model decreases with the increase of the particle's dislodging phase, in other word, the result of the stochastic model is converging to that of the deterministic model with the particle's dislodging phase.

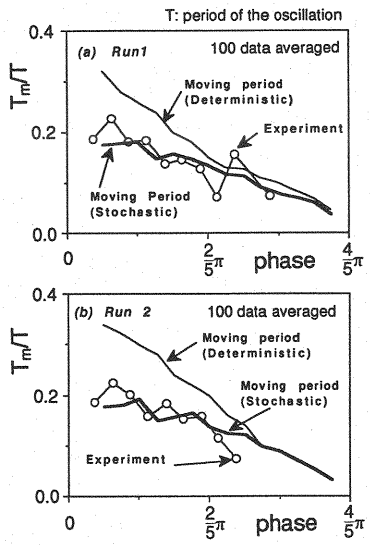

Fig. 6 Mean moving period

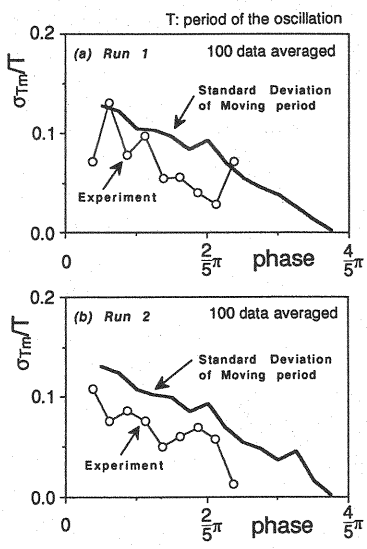

Fig. 7 Standard deviation of moving period

Moving period is determined by the rest event, which is divided into following two subsets: (A) the rest due to the sudden loss of particle's momentum by collision and (B) the rest due to the decrease of hydrodynamic force beneath the threshold of particle's motion. The event (A) is probabilistic, while the event (B) is deterministic. When the particle's dislodging phase is small, the event (A) is dominant, therefore the difference between the result of the deterministic model and that of the stochastic model is large. The decrease of the difference between two models can be explained as the decrease of the effect of probabilistic event (A), as follows. The probabilistic aspect of bed-load transport is mainly brought about by the irregular collision with protrusions on bed. If the spatial distribution of protrusions are statistically uniform, the number of collision decreases with the increase of particle's dislodging phase. Decrease of the number of collisions means the decrease of the effect of probabilistic event (A).

Figure 7 shows the results of the simulation and the experiments on the standard deviation of moving period. Although the results of stochastic simulation tend to overestimate the standard deviation compared with the experimental data, which may correspond to the upper edge of the experimental

results, the general tendencies of the experiments are simulated well by the present stochastic model. Needless to say, the deterministic model cannot estimate the standard deviation at all.

The conditional probability density of moving period against the particle's dislodging phase is shown in Fig. 8. In this figure, the experimental data are also plotted when $\phi_0=(2/10)\pi$, $(3/10)\pi$ and $(4/10)\pi$, in which $\phi_0 \equiv 2\pi(t_0/T)$; and t_0=particle's dislodging time. The result of the numerical simulation shows the following characteristics: The probability density which is widely distributed at early dislodging phase becomes narrower gradually with the increase of dislodging phase, and the distribution, the shape of which is flat, becomes gradually sharp with the increasing dislodging phase. These features are brought about mainly by the relative strength of the probabilistic aspect changing with the dislodging phase of particle. When the probabilistic aspect is intensive, the probability density shows a wide range distribution with flat shape. On the other hand, when the probabilistic aspect is weak, the probability density is narrowly distributed with sharp peek around the deterministic moving period.

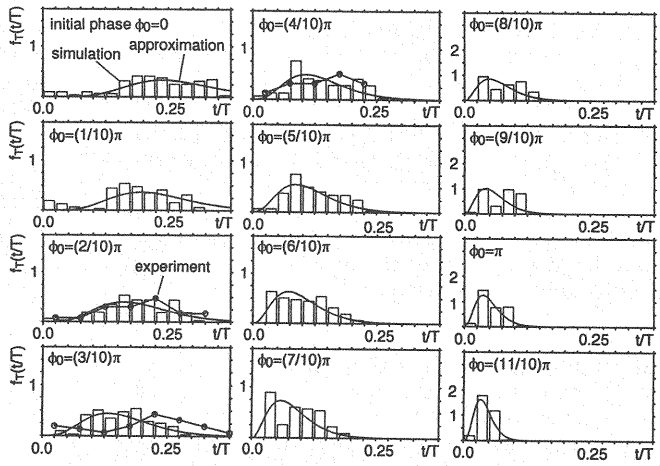

Fig. 8 Probability density of moving period in oscillation-current coexisting flow

The solid curve shown in Fig. 8 is a gamma distribution which approximates the distribution of moving period. It is written as follows:

$$f_T(\xi) = \frac{\lambda}{\Gamma(r)}(\lambda\xi)^{r-1}\exp(-\lambda\xi) \quad ; \quad \xi = \frac{t}{T_m} \tag{12}$$

$$\lambda = \frac{T_m}{\sigma_{T_m}^2} \quad ; \quad r = \left(\frac{T_m}{\sigma_{T_m}}\right)^2 \tag{13}$$

in which T_m, σ_{Tm}=mean and standard deviation of moving period. The result of the simulation can be approximated fairly well by Eqs. 12 and 13.

Figure 9 shows the transformation process from the pick-up rate to the deposit rate formulated as follows:

$$p_d(t) = \int_0^\infty p_s(t-\tau) f_T(\tau|t-\tau)\mathrm{d}\tau \tag{14}$$

in which $p_d(t)$=deposit rate of bed-load particle; $p_s(t)$=pick-up rate of bed-load particle; and $f_T(\tau|t)$= probability density function of moving period of the particle picked up at time t. By letting the experimental results of pick-up rate and the predicted probability density of moving period into Eq. 14, the deposit rate is estimated.

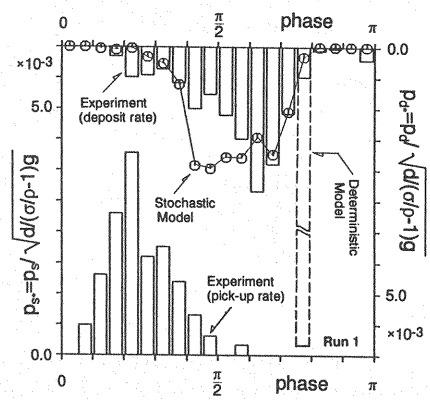

Fig. 9 Transformation process from pick-up rate to deposit rate in oscillation-current coexisting flow : Comparison between sim-ulation and experiment

The changes of the deposit rate simulated by the stochastic model and those calculated by the deterministic model for a given change of pick-up rate are compared with the experiments. The range of the distribution of the deposit rate is accurately estimated by the stochastic model, but the deterministic model cannot estimate the distribution. The result of the experiment indicates that the deposit-rate distribution is skew. Here the falling limb is steeper than the rising one. The result of simulation also shows this

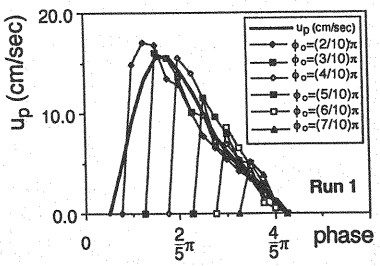

Fig. 10 Speeds of particle

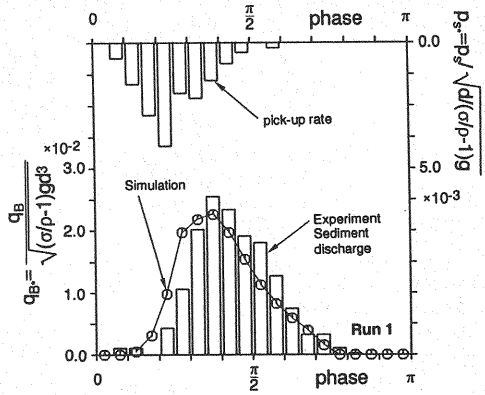

Fig. 11 Seimdnt discharge in oscillation-current coexisting flow

tendency fairly well, though the peek-phase is rather underestimated.

Figure 10 shows the speed of particles calculated by the stochastic model. The solid line in Fig. 10 is the equilibrium speed of particle that is derived from Eq. 7 by putting $du_p/dt=du/dt=0$ and given as follows:

$$u_p = \beta_{up}\left\{u - \frac{2A_3 d}{A_2}\frac{(\sigma/\rho-1)g\alpha_{up}\mu_{f0}}{C_D}\right\} \tag{15}$$

in which α_{up}, β_{up} are empirical constants ($\alpha_{up}=\beta_{up}=0.8$). The coefficient α_{up} is set that the speed of particle is equal to zero at the critical phase of particle's motion, and the coefficient β_{up} implies the decrease of the speed of particle due to the collision with protrusions on bed. Fig. 10 shows that Eq. 15 is a good approximation of the simulation results.

The sediment discharge is formulated as follows :

$$q_B(t) = \frac{A_3 d}{A_2}\int_0^\infty p_s(t-\tau)\cdot u_p(t|t-\tau)\int_\tau^\infty f_T(\zeta|t-\tau)\mathrm{d}\zeta\,\mathrm{d}\tau \tag{16}$$

in which u_p=speed of the particle picked up at time t-τ. By substituting Eq. 15 into the above, Eq. 16 can be written as follows:

$$q_B(t) = \frac{A_3 d}{A_2}\cdot u_p(t)\int_0^\infty p_s(t-\tau)\int_\tau^\infty f_T(\zeta|t-\tau)\mathrm{d}\zeta\,\mathrm{d}\tau \tag{17}$$

Figure 11 shows the change of sediment discharge estimated by applying the simulation results to Eq.17. Although simulation result gives a slight overestimation on the rising limb, the range of the sediment-discharge distribution is fairly well estimated by the simulation. The peek-phase of the simulation result agrees well with the experimental data. Furthermore, the experimental data skews: the rising limb is steeper than the falling one. Such an asymmetry distribution of the sediment-discharge is excellently expressed by the simulation.

APPLICATION OF SIMULATION TO THE BED-LOAD TRANSPORT DUE TO WAVE ACTION

The present simulation is applied to the bed-load transport due to wave action. Sawamoto & Yamashita (7) measured the time series of pick-up rate and deposit rate under wave action, and they found that the pick-up-phase is clearly separated from the deposit-phase. On the other hand, in the oscillation-current coexisting flow treated in the present study, there is an overlap region of the pick-up-phase and deposit-phase. In other words, in the oscillation-current coexisting flow, the dislodgment of certain particles and the rest of other particles may occurs simultaneously. The irregular collision with

the protrusion on bed, which makes the transport process stochastic, causes the simultaneous occurrence of dislodgment and deposition. Therefore, the experimental results indicate that the bed-load motion in the oscillation-current coexisting flow is more widely dominated by the stochastic aspect than that due to wave action.

The application of the present simulation to the bed-load transport due to the wave action makes it possible not only to check the applicability of the present simulation but also to estimate the transport mechanism. In Fig. 12, the experimental data are compared with the results of stochastic simulation. The result of deterministic calculation by Sawamoto & Yamashita is also shown in this figure. In this calculation, the μ_f is set 0.4, and the coefficient to express the imperfectly elastic collision with protrusion β_1 is set 0.05, in order to fit the result of the simulation to the experimental data. The coefficient μ_f expresses the strength of the contact of moving particle to a bed in the moving process, while the coefficient β_1 expresses the strength of the imperfectly elastic collision which makes the transport process probabilistic. In this calculation, both of the coefficients are set smaller than those of the oscillation-current coexisting flow. This fact means that the contact between moving particle and a bed under the wave action is smaller than that in oscillation-current coexisting flow, and that the probabilistic aspect, which dominates the sudden rest of the particle caused by collision with protrusions on bed, is smaller in the wave action than that in the oscillation-current coexisting flow.

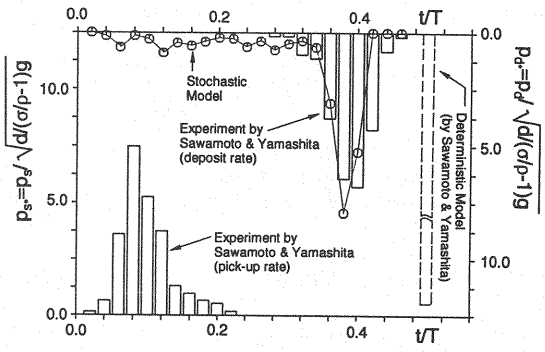

Fig. 12 Transformation process from pick-up rate to deposit rate due to wave action: Comparison between simulation and experiment

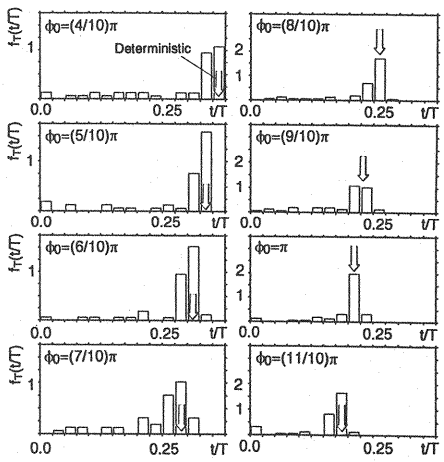

Fig. 13 Probability density of moving period

The agreement between the stochastic simulation and the experimental results is good. Although, at the early phase, the deposit rate is not experimentally observed, the stochastic simulation predicts a small deposit rate. The peek-height and -phase of the deposit rate estimated by the stochastic simulation show fairly good agreements with the experiments; while the deterministic approach cannot express the deposit-rate distribution.

Figure 13 shows the probability density of moving period estimated by the present simulation under the condition of the experiments by Sawamoto & Yamashita. The asymmetry of the probability density is more appreciable than that in the oscillation-current coexisting flow, namely the probability density has a small value in an early phase, and suddenly rises up just before the deterministic moving period, and after passing the sharp peek, it rapidly falls down to zero. This tendencies of the simulated probability density function also leads to the same conclusions mentioned above, namely the effect of the probabilistic aspect in the bed-load motion due to wave action is smaller than that in the oscillation-current coexisting flow.

CONCLUSIONS

The results obtained in this paper are summarized as follows:

(1) The motion of bed-load particle was investigated with the aid of the numerical simulation, by dividing the bed-load transport process into two subprocesses: the moving process, in which the particle is traced by the equation of a sliding motion; and the collision process with protrusions on bed, in which the effect of the probabilistic characteristics of protrusion's height is taking into account. By applying the simulation model of the bed-load transport in oscillation-current coexisting flow, the characteristics of the moving period has been estimated. A good agreement of the simulation with the experiment was

recognized.

(2) The probability density of moving period, the detail of which is difficult to be investigated by experiment, was estimated by the numerical simulation. The extent how sensitively the bed-load transport process depends on the probabilistic aspect varies with the dislodging phase of particles.

(3) The transformation process from pick-up rate to deposit rate was estimated by letting the simulated probability density of moving period into the convolution-integral formed bed-load transport formula. The stochastic simulation can estimate the deposit rate distribution, with sufficient accuracy; while the deterministic approach cannot estimate the deposit rate distribution. The advantage of the stochastic simulation over the deterministic one is confirmed.

ACKNOWLEDGMENTS

The authors express their sincere gratitude to Mr. Masaru Senba (graduate student, Kyoto University) for his help in the experimental data processing.

REFERENCES

1. Einstein, H.A. : The bed-load function for sediment transportation in open channel flows, Tech. Bull., U.S. Dep. Agri., Soil Conservation Service, No. 1025, 1950.
2. Nakagawa, H. and Tsujimoto, T. : Sand bed instability due to bed load motion, *J. Hydraul. Div.*, ASCE, Vol.106, HY12, pp.2029-2051, 1980.
3 Nakagawa, H. and Tsujimoto, T. : *Mechanics of Sediment Transport and Alluvial Hydraulics*, Gihodo Shuppann, Tokyo, 320p., 1986 (in Japanese).
4. Nakagawa, H., Tsujimoto, T. and Gotoh, H. : Stochastic model of bed-load movement in oscillation-current coexisting flow, *Ann., Disas. Prev. Res. Inst., Kyoto Univ.*, No. 33 B-2, pp.595-603, 1990 (in Japanese).
5. Nakagawa, H., Tsujimoto, T. and Hosokawa, Y.: Stochastic study on origin of small scale bed forms related to probabilistic characteristics of bed load movements, *Proc. 3rd Int. Sym. on Stochastic Hydraulics*, Tokyo, Japan, pp.359-370, 1980.
6. Tsujimoto T. and Nakagawa, H. : Stochastic study on successive saltation by flowing water, *Proc. 2nd Int. Sym. on River Sedimentation*, pp.173-186, Nanjing, Chaina, 1983.
7. Sawamoto, M. and Yamashita, T. : Sediment transport rate due to wave action, *Jour. HydroSci. Hydr. Eng.*, Vol. 4, No. 1, pp. 1-15, 1986.
8. Sekine, M. and Kikkawa, H. : Rest mechanism of the transported particles as bed-load, *Proc. JSCE*, No.399, pp.105-112, 1988 (in Japanese).

APPENDIX-NOTATION

The following symbols are used in this paper:

A_2, A_3 = two-and three-dimensional geometrical coefficients of particle, respectively;
B_* = constant in the equation of the collision;
C_M = added mass coefficient;
C_D = drag coefficient;
d = diameter of particle;
$f_T(\zeta|t)$ = probability density function of the moving period of the particle picked up at a time t;
$f_H(\Delta)$ = probability density function of the height of the protrusion;
$f_{Tm}(\xi)$ = approximated distribution of the simulated probability density function of the moving period;
g = gravitational acceleration;
$h(u_{out}|u_{in})$ = transition probability of the particle's speed by collision with the protrusion;
I_G = moment of inertia;
M = virtual mass of the particle;
t_0 = dislodging time of the particle;

T = period of oscillation;
u = flow velocity;
u_{in}, u_{in*} = speed of the particle just before the collision and its dimensionless form;
u_{out}, u_{out*} = speed of the particle after the collision and its dimensionless form;
u_p = speed of the particle;
$p_s(t)$ = pick-up rate of bed-material particle;
$p_d(t)$ = deposit rate of bed-load particle;
T_m = mean moving period;
x_p = longitudinal coordinate in the equation of particle's motion;
x_{pr} = mean interval of neighboring protrusions;
α = variation coefficient of the protrusion's spacing;
α_{up} = empirical constant in the equation with respect to the particle's speed equation;
α_x = variation coefficient of interval of neighboring protrusions;
β_1 = coefficient of the imperfectly elastic collision;
β_{up} = empirical constant in the equation with respect to the particle's speed equation;
Δ, Δ_* = height of the protrusion and its dimensionless form;
ϕ_0 = dislodging phase of the particle;
μ_f, μ_{f0} = coefficients of kinetic- and static friction, respectively;
ρ = mass density of fluid;
σ = mass density of bed-material particle; *and*
σ_{Tm} = standard deviation of the protrusion's height.

(Received January 7, 1992; revised April 15, 1993)